

IMPROVED LIFETIME FOR LARGE AREA INVERTED ORGANIC SOLAR CELLS, USING A NOVEL ENCAPSULATED METHOD

D. CHALAL^{1,2}, B. RATIER¹, D. BENACHOUR²

¹XLIM UMR 7252, Université de Limoges/CNRS, 123 Avenue Albert Thomas
87060 Limoges Cedex, France.
b.ratier@xlim.fr.

²Université Ferhat Abbas Sétif 1, Sétif 19000, Algérie.
chalal.djazia@yahoo.fr

ABSTRACT

In this paper, we study the performance and stability of solution-processed inverted organic solar cells based on photoactive blends composed by the conjugated regioregular poly-(3-hexylthiophene) (P3HT) and [6,6]-phenyl-C61-butyric acid methyl ester (PCBM), using an active area of 2 cm². These inverted organic solar cells are fabricated with a novel top electrode design in which the silver electrode is deposited over the whole substrate to completely cover the photoactive layer, allowing an effective protection of the entire device. Consequently, initial power conversion efficiencies of 3.2% are maintained at 95% after 15h under standard illumination conditions in ambient.

These IOSCs are fabricated with a novel encapsulation method in which the Ag metal top electrode was deposited over the whole ITO substrate to cover completely the photoactive layer, which allowed effective protection of the entire device. PCEs are maintained to 95% and 1 % of the initial values for the encapsulate and the un-encapsulate device respectively when exposed to air and light for 15h. Conclusively, we find that the encapsulated device exhibit much higher stability than the un-encapsulated device.

Keywords: *Inverted Organic solar cells, Degradation, Stability, Lifetime.*

NOMENCLATURE

Symbols :

J_{sc}, short circuit current, mA/cm²
V_{oc}, open circuit voltage, V
FF, fill factor
R_s, serie resistance, Ω
R_{sh}, shunt resistance, Ω
PCE, photoconversion efficiency ,%

Subscripts :

Au, gold
Ag, silver
OPV organic photovoltaics
PV photovoltaic parameters
IOSCs Inverted Organic Solar Cells
AM1.5G, standard solar spectrum at the Earth's surface

1. INTRODUCTION

Intensive research has been carried out to understand degradation mechanisms [1, 2] and improve the stability of polymer organic solar cells [3,4]. Stability is an essential issue in polymer solar cells for achieving commercially applicable devices [5]. The device architecture of Inverted Organic Solar Cells (IOSCs) has attracted much attention recently due to the long life time without performance degradation of these IOSCs [6]. The advantage of IOSCs is related to the relative environmental stability of the oxide metal

electron transport layer (e.g. ZnO, TiO₂) and Ag hole-collecting contact. Degradation of OSCs is mostly caused by diffusion of water and moisture in the device through pinholes or grain boundaries of the outer electrode [7–9, 10]. In addition, the deposition of metal leads to its diffusion in the active layer; this will induce reaction with the polymer and alters its semiconducting properties [11, 12]. The degradation mechanism for organic devices is a two stage process: first a rapid decrease, a fast initial drop, followed by a linear degradation as reported in a large number of articles [13-15]. To overcome this problem, several strategies can be employed to improve the device stability like inserting a buffer layer between the active layer and the metal. The most effective approach is to adopt encapsulation techniques that prevent or limit the exposure of organic electronic devices to water vapor and oxygen. Many studies regarding the encapsulation method that can protect organic devices from these aggressive agents, have been conducted [16]. The best encapsulation process was reported in 2007, where the PCE drops by 6% after 6145 h. This encapsulation method is rather complicated since it used atomic layer deposition (ALD) technique [17].

In the present paper, we have fabricated efficient and stable inverted solar cells based on solution processing of P3HT:PCBM, with a large active area of 2cm². In order to enhance the stability of this device, a new encapsulated model was applied. The active layer was entirely covered by a silver layer (anode top contact layer) until ITO substrate edges. With this architecture all devices have retained their power efficiency without apparent degradation. The encapsulated devices were very stable and have retained more than 95% of their original efficiency over an extended measurement period up to 15 h, under continuous illumination in air. The aim of this novel cell architecture, self or auto-encapsulation, was not only to enhance stability, but also to avoid the need for insertion or introduction of ultra-barrier organic/inorganic multilayer to the device, thus reducing the solar fabrication cost.

2. EXPERIMENTAL

In our organic BHJ inverted solar cells, indium tin oxide (ITO)-coated glass substrates purchased from (Vision-Tech) with a sheet resistance of 7/sq, were patterned by wet chemical etching to define rectangular design area of 2cm². First S Ω amples with 2,5× 2,5 cm² were cleaned by successive sonification in detergent, de-ionized (DI) water, acetone, ethanol and IPA for 10 min each followed by the treatment of ultraviolet ozone for 10 min. Before layer deposition, Au and Ag stripes with thickness of 60 nm were deposited separately onto cleaned ITO through a mask by thermal evaporation and ion beam sputtering (IBS) [18-21] respectively for the sub- electrode. Ag stripe was deposited using Ag target with 99,99% purity where the sample of ITO was placed at a distance of 6 cm from the target and oriented with respect to its axis at 60° resulting in growth rate of 1,6 nm/min. Sputtering was carried out at a pressure of 4x10⁻⁴Pa in the vacuum chamber at a power of 6 keV with a current density of about 1 mA/cm². Pure argon gas was used as the sputtering gas. Gold and silver sub-electrodes work as conducting electrodes, in order to reduce the resistive loss of ITO [22]. Afterwards ZnO nano-particules-suspension, purchased from Genes Ink (ZnO 5F2) used as electron injecting layer, was spin coated on the substrate and annealed on a hot plate at 130°C for 10 min in air. The photoactive layer was formed from a blended solution of P3HT:PCBM (from BASF and American Dye Source respectively). P3HT and PCBM were dissolved in ortho-dichlobenzene (Sigma–Aldrich) (CARLOERBA) with a ratio of 1:0.8 by weight. The solution was stirred inside the glove box at 50°C during one night and filtered with (PTFE 0,2µm) before processing. The photoactive layer was spin coated in a nitrogen glove box at 780 rpm for 40s, giving a 220 nm thick layer, and subsequently dried at 50°C for 15min. A 40 nm thick layer of PEDOT:PSS (from Heraeus, RD CLEVIOS F010) was spin coated on top of the P3HT:PCBM layer in air after passing through (0.45µm) filter. Subsequently, a 100 nm-thick silver top electrode was deposited by thermal evaporation through a shadow mask at a pressure of about 10–6 bar to yield a device area of 2cm². Finally, the complete device was annealed at 110 °C for 30min under inert conditions. The device structure is shown in Fig 1.

The (J-V) characteristics were measured using SMU 2400 Keithly source meter unit under illumination of solar simulator (Atlas Solar Constant 575 PV) with 100mW/cm² AM 1,5G spectrum. The calibration of the light intensity was performed using a standard Si photodiode cell. Film thicknesses were measured using a

Bruker Dektak XT profiling system [23]. The ageing process was performed in ambient air under continuous illumination with intensity of 100 mw/cm^2 , the devices were kept at a temperature of $48 \text{ }^\circ\text{C}$ and tested every 5min for a total duration of 20 h [14].

3. RESULTS

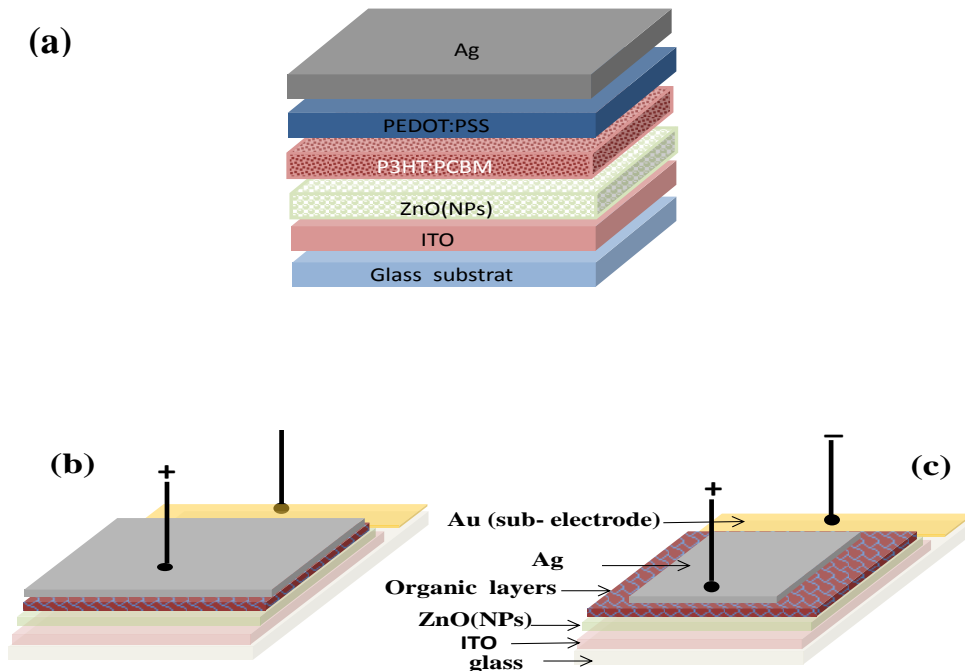


FIGURE1 .(a) structure of inverted architecture solar cell, (b) encapsulated design with Au sub-electrode, (c) un-encapsulated design with Au sub-electrode. The polymer layers are PEDOT:PSS and P3HT:PCBM layers.

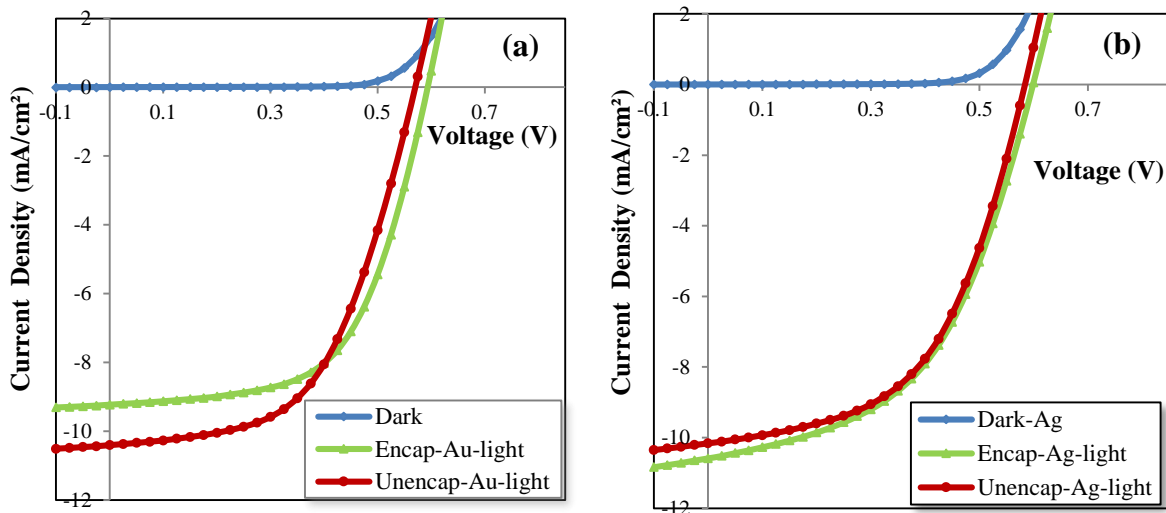


FIGURE 2. Current density versus voltage (J–V) characteristics of inverted organic solar cells fabricated with: (a) gold sub-electrode, and : (b) silver sub-electrode as cathode contact. All measurements were performed under AM 1.5 illumination conditions (100 mW/cm^2).

Fig.2 shows the J-V characteristics of the inverted solar cells as fabricated, realized with encapsulated and un-encapsulated architectures. These cells with an active area of 2 cm^2 , exhibit a power efficiency up to 3%

for the different devices. IOSCs with silver sub-electrode show a short circuit current density (J_{sc}) of 10.55 mA/cm², an open circuit voltage (V_{oc}) of 0.58V, a fill factor (FF) of 0.51 and a PCE of 3.16%, while for cells with gold sub metal electrode the performances were: ($J_{sc} = 9.22$, $V_{oc}=0.59$, $FF=0.59$ and $PCE=3.25\%$). The devices with gold display the best efficiency attributed to the low series resistance and high shunt resistance which, probably, are due to the high conductivity of gold metal. As presented in Fig 2 the device with silver sub-electrode exhibits a low leakage current, this is not observed on gold sub electrode anode side indicating a more effective electron collection. However, metal sub-electrodes are used to reduce series resistance (R_s) and to improve device performance for large areas [22,26]. The PCEs were practically the same for ($n>30$) of encapsulated and un-encapsulated devices as fabricated due to the high homogeneity in the active layer by the spin coating process. This method can be used to evaluate the large area IOSCs with high performance. The values of the photovoltaic characteristic before encapsulation and after encapsulation are given in Table 1. The results were similar which means that no significant negative change in the device performance was observed after encapsulation.

Devices	J_{sc} (mA/cm ²)	V_{oc} (V)	FF	η (%)	R_s (Ω)	R_p (Ω)
Encapsulated with Au sub -electrode	9,22	0,59	0,59	3,25	6,75	541,24
Non-encapsulated with Au sub electrode	10,4	0,57	0,55	3,23	7,51	408,38
Encapsulated with Ag sub -electrode	10,55	0,58	0,51	3,16	8,02	198,29
Nonencapsulated with Ag sub -electrode	10,16	0,58	0,53	3,11	7,89	247,63

Table 1. PV parameters for the encapsulated and un-encapsulated inverted devices with gold (or and) silver sub-electrode used as cathode. (more than 30 devices were tested).

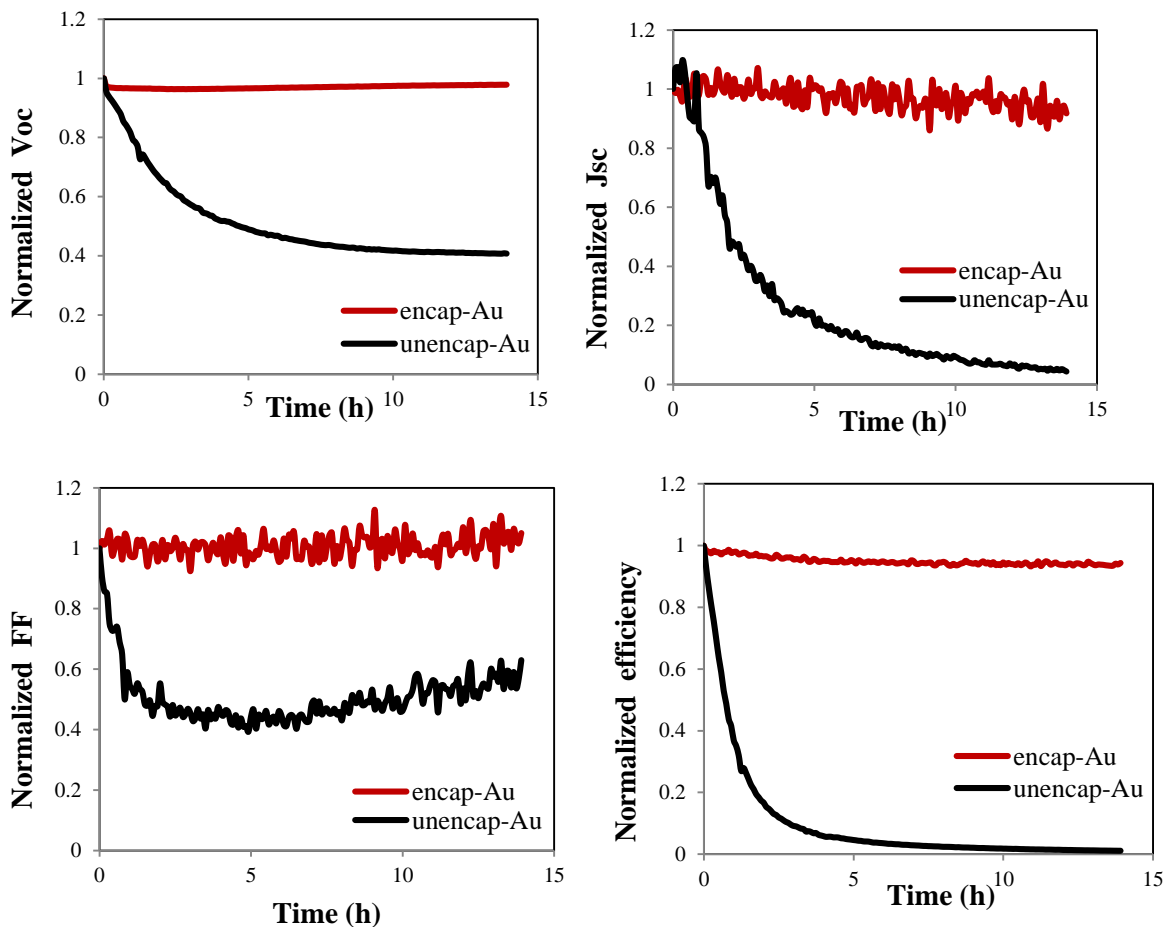


FIGURE 3. Normalized PV parameters for an inverted device with encapsulation (red) and without encapsulation (black) as a function of light exposure time. All devices were fabricated with a gold (Au)sub-electrode as cathode contact

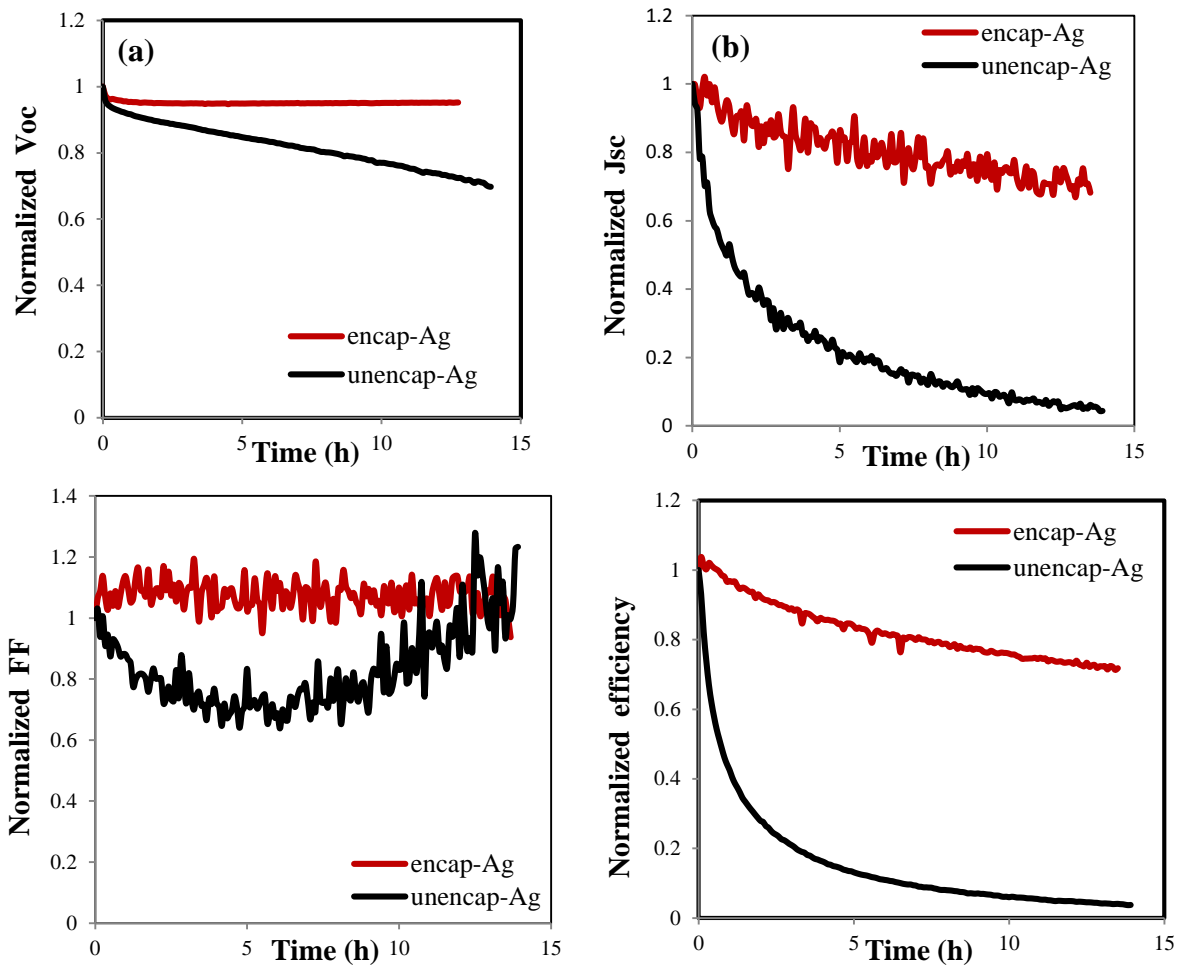


FIGURE 4. Normalized PV parameters for an inverted device with encapsulation (red) and without encapsulation (black) as a function of light exposure time. All devices were fabricated with silver (Ag) sub-electrode as cathode contact.

Identification of the mechanism that causes degradation is done through the study of the evolution of the cell parameters with time. The stabilities of the cells, with and without encapsulation, are shown in (Fig. 3 and 4). Photovoltaic characteristics were measured under AM 1.5 G 1 sun light intensity of 100 mW/cm² and normalized to their initial values. Ageing process was studied in ambient air under continuous illumination at regular intervals. Temperature of the immediate cell environment was kept at 48°C. The performance parameters were compared to their initial values as a function of exposure time, in ambient atmosphere, to investigate the effectiveness of the encapsulation.

Fig.3 shows the relative change of (Voc), (Jsc), (FF) and (PCE) for encapsulated and un encapsulated devices over 20h of exposure time. In the case of the un encapsulated devices, we observed a rapid drop in Voc during the first 2h, then a continuous linear decrease for the remainder duration of the test, while the FF decreases rapidly at the beginning then increases slightly from 55% to 59% after 8h of exposure, followed by a steady increase until the end of the measurement. The drop of the FF is correlated with an increase of the series resistance indicating a reduced charge extraction due to the photo degradation of the organic- electrode interfaces [25]. On the other hand, (Jsc) and (PCE) decrease by about 53% and 80% respectively after 2h exposure, then these two parameters continue to decrease until approaching zero. In contrast with encapsulated device (Voc) and (FF) remain still unchanged over the time of test. It was noted that, particularly (Jsc) decreased very slowly and lost only 5% of its initial performance, thus we may conclude that the device retains its efficiency without degradation even after 15h of exposure time. The

reductions in VOC, FF, JSC and PCE were 2.05 %, 5.5%, 8.04%, and 5.61%, respectively, for the encapsulated devices with gold sub metal contact cathode. On the other hand, these four characteristics decreased by 59.20%, 36.92%, 95.61% and 98.87%, respectively in the case of the un-encapsulated devices. These results indicate the effective device stability achieved through the auto-encapsulation technique we used. As a consequence, the use of the silver anode as a protecting layer will be more appropriate for prolonging the IOSCs life time.

Fig.4 shows the stability plots over time for IOSCs fabricated with silver sub-electrode as cathode contact. The behavior of the encapsulated cells differs from that of the un-encapsulated ones: (Voc) and (FF) remained relatively stable; however, (Jsc) and PCE changed a little at the beginning then decreased by 20% and 15% respectively after 20h of exposure time. For the un-encapsulated devices, the photocurrent dropped sharply during the initial period (up to 4h) and continued to decrease to a lower level until catastrophic failure, causing a large decrease of about 90% in (PCE). From all the above measurements, two distinct degradation mechanisms were observed as already reported in the literature [15]. First, an initial exponential decay in (Jsc) caused by diffusion of water through pinholes or grains in the silver anode, followed by a second catastrophic current loss after a prolonged test duration[18], characterized by a plateau in the degradation curve to indicate a uniform deterioration in the whole active layer of the device. The degradation decay was similar for all the un-encapsulated devices using Ag or Au metal sub-electrode.

Water diffusion through pinholes in silver electrode. H₂O dissociates into H⁺ and OH⁻ ions acting to locally de-dope PEDOT:PSS to a non-conducting state [24]. The first drop in PCE due to the drop in Jsc could be mainly caused by the oxidation of the PEDOT:PSS which leads to the loss of its conductivity, resulting in an increased series resistance and a local delamination of the PEDOT:PSS-Ag interface can occur [18]. In order to elucidate the difference which occurs in photocurrent degradation between the inverted encapsulated and the un-encapsulated devices, a laser beam-induced current mapping system was used to control the photocurrent degradation within the active area of the device.

4. CONCLUSION

We have demonstrated that highly air-stable inverted solar cells can be obtained by the use of a novel encapsulation method. The encapsulated devices have retained 95% of their efficiency even after 20h of exposure, under continuous illumination in air. Encapsulated and un-encapsulated devices, fabricated with a large active area of 2 cm², showed a high power conversion efficiency up to 3.2%. All photovoltaic parameters (short-circuit current density, fill factor, and conversion efficiency) for the inverted solar cells with encapsulation, revealed more stability than those without encapsulation. The new encapsulation technique with the silver back electrode layer was effective to improve the stability of the devices because of the more effective protection for the device exposed to ambient air. The novel encapsulation process acts in blocking the diffusion of water and oxygen within the photoactive active layer through the pinholes and edges of the top electrode. This approach can be useful to improve the lifetime of the IOSCs in future commercial applications.

REFERENCES

- [1] F.C. Krebs, K. Norrman, Prog. Photovoltaics 15, 697, (2007)
- [2] M. Jorgensen, K. Norrman, F.C. Krebs, Sol. Energy Mater. Sol. Cells 92, 686, (2008).
- [3] D.H. Wang, S.H. Im, H.K. Lee, O.O. Park, J.H. Park, J. Phys. Chem. C 113, 17268, (2009).
- [4] K. Lee, J.Y. Kim, S.H. Park, S.H. Kim, S. Cho, A.J. Heeger, Adv. Mater. 19, 2445, (2007).
- [5] P.C. Yang, J.Y. Sun, S.Y. Ma, Y.M. Shen, Y.H. Lin, C.P. Chen, C.F. Lin, Interface modification of a highly air-stable polymer solar cell, Sol. Energy Mater. & Sol Cells 98, 351–356, (2012).
- [6] Y.J. Kang, K. Lim, S. Jung, D.G. Kim, J.K. Kim, C.S. Kim, S.H. Kim, J.W. Kang, spray-coated electron transport layer for air stable inverted organic solar cells, Sol. Energy Mater. & Sol Cells 96, 137–140, (2012).
- [7] K. Norrman, N.B. Larsen, F.C. Krebs, Lifetimes of organic photovoltaics: combining chemical and physical characterization techniques to study degradation mechanisms, Sol. Energy Mater. Sol. Cells 90, 2793–2814, (2006).

- [8] M. Jorgensen, K. Norrman, F.C. Krebs, Stability/degradation of polymer solar cells, *Sol. Energy Mater. Sol. Cells* 92, 686–714, (2008).
- [9] M. Boman, S. Stafstrom, and J. L. Bredas, *J. Chem. Phys.* 97, 12, (1992).
- [10] J. Birgersson, M. Fahlman, P. Broms, and W. R. Salaneck, *Synth. Met.* 80, 125, (1996).
- [11] F.C. Krebs, K. Norrman, Analysis of the failure mechanism for a stable organic photovoltaic during 10,000 h of testing, *Prog. Photovolt.: Res. Appl.* 15, 697–712, (2007).
- [12] K. Norrman, S.A. Gevorgyan, F.C. Krebs, Water-induced degradation of polymer Solar cells studied by H₂¹⁸O labeling, *Appl. Mater. Interfaces* 1, 102–112, (2009).
- [13] E. Voroshazi, B. Verreert, A. Buri, R. Müller, D. Di Nuzzo, P. Heremans, Influence of cathode oxidation via the hole extraction layer in polymer: fullerene solar cells, *Organic Electronics*, 12, 736–744, (2011).
- [14] Y. Lare, B. Kouskoussa, S. Ouro Djoko, K.L. Cattin, F.R. Diaz, Influence of exciton blocking layer on the stability of layered organic solar cells. *Journal of Physics and Chemistry of Solids*, 72, 97–103, (2011).
- [15] X. Wang, C.X. Zhao, Gu. Xub, Z.-K. Chena, F. Zhu. Degradation mechanisms in organic solar cells: Localized moisture encroachment and cathode reaction, *Sol. Energy Mater. Sol. Cell*, 104, 1–6, (2012).
- [16] M. Tavakkoli, R. Ajeian, M.N. Badrabi, S.S. Ardestani, S.M. Hasan Feiz, K. Elahi, Nasab Progress in stability of organic solar cells exposed to air *Sol. Energy Mater. Sol. Cells*, 95, 1964–1969, (2011).
- [17] H.J. Lee, H.P. Kim, H.M. Kim, J.H. Youn, D.H. Namb, Y.G. Lee, Solution processed encapsulation for organic photovoltaics, *Sol. Energy Mater. Sol. Cells*, 111, 97–101, (2013).
- [18] M.T. Lloyd, G.H. Peters, A. Garcia, I.V. Kauvar, J. J. Berry, M.O. Reese, M.D. McGehee, D.S. Ginley, D.C. Olson, Influence of the hole-transport layer on the initial behavior and lifetime of inverted organic photovoltaics, *Sol. Energy Mater. Sol. Cells*, 95, 1382–1388, (2011).
- [19] A. El Hajj, B. Lucas, M. Chakaroun, R. Antony, B. Ratier, M. Aldissi, Optimization of ZnO/Ag/ZnO multilayer electrodes obtained by Ion Beam Sputtering for optoelectronic devices, *Thin Solid Films*, 5204, 666–4668, (2012).
- [20] B. Lucas, W. Rammal, A. Moliton, ITO films realized at room temperature by ion beam sputtering for high-performance flexible organic light-emitting diodes, *The European Physical Journal Applied Physics*, 34, 179–187, (2006).
- [21] D. Kim, Y. Han, J.-S. Cho, S.-K. Koh, Low temperature deposition of ITO thin films by ion beam sputtering, *Thin Solid Films*, 81–86, 377–378, (2000).
- [22] S.Y. Park, Y.J. Kang, S. Lee, D.G. Kim, J.K. Kim, J.H. Kim, J.W. Kang, Spray coated organic solar Cells with large-area of 12.25 cm², *Sol. Energy Mater. Sol. Cells*, 95, 852–855, (2011).
- [23] S. Vedraïne, A. El Hajj, P. Torchio, B. Lucas Optimized ITO-free tri-layer electrode for organic solar cells, *Organic Electronics*, 14, 1122–1129 (2013).
- [24] J. Kim, P. Ho, C. Murphy, N. Baynes, R.H. Friend, Nature of non-emissive black spots in polymer light-emitting diodes by in-situ micro-Raman spectroscopy, *Adv. Mater.* 14, 206–20, (2002).
- [25] E. Voroshazi, B. Verreert, T. Aernouts, P. Heremans, Long-term operational lifetime and degradation analysis of P3HT: PCBM photovoltaic cells, *Sol. Energy Mater. Sol. Cells* 95, 1303–1307, (2011).
- [26] J.W. Kang, Y.J. Kang, S. Jung, M. Song, D.G. Kim, C. Su Kim, S. Kim, Fully spray-coated inverted organic solar cells, *Sol. Energy Mater. Sol. Cells*, 103, 76–79 (2012).